Genome location dictates the transcriptional response to PolC inhibition in Clostridium difficile

Eijk, E. van; Boekhoud, I.M.; Kuijper, E.J.; Bos-Sanders, I.M.J.G.; Wright, G.; Smits, W.K.

AMERICAN SOCIETY FOR MICROBIOLOGY | Antimicrobial Agents and Chemotherapy®

Genome Location Dictates the Transcriptional Response to PolC Inhibition in *Clostridium difficile*

Erika van Eijk,[a] Ilse M. Boekhoud,[a,b,c] Ed J. Kuijper,[a,c] Ingrid M. J. G. Bos-Sanders,[a] George Wright,[d] Wiep Klaas Smits[a,b,c]

[a]Department of Medical Microbiology, Center for Infectious Diseases Leiden University Medical Center, Leiden, the Netherlands
[b]Centre for Microbial Cell Biology, Leiden, the Netherlands
[c]Netherlands Centre for One Health‡
[d]Acurx Pharmaceuticals, White Plains, New York, USA

ABSTRACT *Clostridium difficile* is a potentially lethal gut pathogen that causes nosocomial and community-acquired infections. Limited treatment options and reports of reduced susceptibility to current treatment emphasize the necessity for novel antimicrobials. The DNA polymerase of Gram-positive organisms is an attractive target for the development of antimicrobials. ACX-362E [N^2-(3,4-dichlorobenzyl)-7-(2-[1-morpholinyl]ethyl)guanine; MorE-DCBG] is a DNA polymerase inhibitor in preclinical development as a novel therapeutic against *C. difficile* infection. This synthetic purine shows preferential activity against *C. difficile* PolC over those of other organisms *in vitro* and is effective in an animal model of *C. difficile* infection. In this study, we have determined its efficacy against a large collection of clinical isolates. At concentrations below the MIC, the presumed slowing (or stalling) of replication forks due to ACX-362E leads to a growth defect. We have determined the transcriptional response of *C. difficile* to replication inhibition and observed an overrepresentation of upregulated genes near the origin of replication in the presence of PolC inhibitors, but not when cells were subjected to subinhibitory concentrations of other antibiotics. This phenomenon can be explained by a gene dosage shift, as we observed a concomitant increase in the ratio between origin-proximal and terminus-proximal gene copy number upon exposure to PolC inhibitors. Moreover, we show that certain genes differentially regulated under PolC inhibition are controlled by the origin-proximal general stress response regulator sigma factor B. Together, these data suggest that genome location both directly and indirectly determines the transcriptional response to replication inhibition in *C. difficile*.

KEYWORDS *Clostridium difficile*, DNA polymerase inhibitor, PolC, RNA-Seq, gene dosage, marker frequency analysis, sigma factor, stress response

Clostridium difficile (*Clostridioides difficile* [1]) is a Gram-positive anaerobic bacterium that can asymptomatically colonize the intestine of humans and other mammals (2–4). However, when the normal flora is disturbed, *C. difficile* can overgrow and cause fatal disease, as has been dramatically demonstrated in the Stoke Mandeville Hospital outbreaks in 2004 and 2005 (5). The ability to form highly resistant endospores coupled to its extensive antibiotic resistance have contributed to its success as a nosocomial and community-acquired pathogen (2–4). Recent years have seen an increase in the incidence and severity of *C. difficile* infections (CDI) due to the emergence of certain PCR ribotypes (3, 6). Antibiotic use is a well-established risk factor for CDI (7), and the emergence of the epidemic PCR ribotype 027 has been linked to fluoroquinolone resistance (8). At present, two antibiotics, metronidazole and vancomycin, are commonly used to treat CDI, and a third, fidaxomicin, is indicated for the treatment of

Citation van Eijk E, Boekhoud IM, Kuijper EJ, Bos-Sanders IMJG, Wright G, Smits WK. 2019. Genome location dictates the transcriptional response to PolC inhibition in *Clostridium difficile*. Antimicrob Agents Chemother 63:e01363-18. https://doi.org/10.1128/AAC.01363-18.

Address correspondence to Wiep Klaas Smits, w.k.smits@lumc.nl.

E.V.E. and I.M.B. contributed equally to this study.

‡ For this virtual institution, see https://ncoh.nl/.

Received 5 July 2018
Returned for modification 14 August 2018
Accepted 4 November 2018
Accepted manuscript posted online 19 November 2018
Published 29 January 2019

relapsing CDI (9, 10). Clearly, limited treatment options and reports of reduced susceptibility to current treatment (11–13) emphasize the necessity for the development of novel antimicrobials and a better understanding of tolerance and resistance to existing therapeutics.

It is increasingly realized that off-target effects that occur when cells are exposed to antimicrobials can contribute to their efficacy but also facilitate the emergence of tolerance and/or resistance (14). Antimicrobials may act as signaling molecules which modulate gene expression (14). Additionally, in particular, those targeting DNA replication (such as polymerase inhibitors) can cause transcriptional effects as a result of differences in gene dosage (15).

The polymerase of Gram-positive organisms is an attractive target for the development of novel antimicrobials (16). First, these PolC-type polymerases are absent from Gram-negative organisms and humans (17, 18). HPUra, one of the first such compounds, is therefore highly active against a wide range of Gram-positive bacteria but does not affect Gram-negative bacteria (17, 18). Template-directed elongation is blocked by the inhibitor through simultaneous binding to the cytosine of the DNA strand and near the active site of PolC. Second, compounds can be derived that have an increased specificity toward specific microorganisms. ACX-362E (Fig. 1) is a compound in preclinical development as a novel therapeutic against *C. difficile*, as it shows preferential activity against *C. difficile* PolC over those of other organisms *in vitro* (19, 20) and will progress to clinical trials in the near future (Acurx Pharmaceuticals, personal communication). PolC inhibitors can cause a stress response and cell death after prolonged exposure. In *Bacillus subtilis*, this stress is characterized by a combination of DNA damage (SOS) response and an SOS-independent pathway dependent on the DNA replication initiator DnaA (21, 22). In *Streptococcus pneumoniae* cells, devoid of an SOS response, competence for genetic transformation is induced upon replication stress (23). The response of *C. difficile* to this particular class of compounds is unknown.

In this study, we characterized aspects of the action of PolC inhibitors toward *C. difficile*. MICs for HPUra and ACX-362E were determined using agar dilution for a large collection of clinical isolates. Next, we investigated the effects of subinhibitory levels of PolC inhibitors on the growth of *C. difficile* in liquid medium and performed RNA sequencing (RNA-Seq) analyses to determine the transcriptional response to PolC inhibitors in our laboratory strain 630Δ*erm*. Finally, marker frequency analysis and transcriptional reporters were used to provide a mechanistic explanation for the observed upregulation of origin-proximal genes under conditions of replication inhibition.

RESULTS

ACX-362E is a potent inhibitor of diverse clinical isolates of *C. difficile*. To date, reports on the activities of PolC inhibitors toward *C. difficile* are limited. MICs have been published for only 4 (19) and 23 (20) *C. difficile* strains, and no analysis was performed on possible differences in efficacy between various phylogenetic groups (24, 25). Therefore, we assessed the sensitivities of a diverse collection of *C. difficile* clinical isolates toward PolC inhibitors and determined if ACX-362E was indeed superior to the general PolC inhibitor HPUra.

HPUra and ACX-362E were tested by the agar dilution method, according to Clinical and Laboratory Standards Institute (CLSI) guidelines for the testing of antimicrobial susceptibility of anaerobes (26, 27), against 363 *C. difficile* clinical isolates collected earlier in the framework of a pan-European study (6, 28).

We found that ACX-362E (MIC_{50}, 2 μg/ml; MIC_{90}, 4 μg/ml) demonstrates lower inhibitory concentrations than the general Gram-positive PolC inhibitor HPUra (MIC_{50}, 16 μg/ml; MIC_{90}, 32 μg/ml) (Fig. 2; see also Table S1 in the supplemental material), consistent with previous *in vitro* activities observed against purified PolC (19). We observed no significant difference in ACX-362E susceptibilities between clades (Table 1), and the different PCR ribotypes demonstrated a similar distribution in MIC values (data not shown). No growth at the highest concentration of compounds

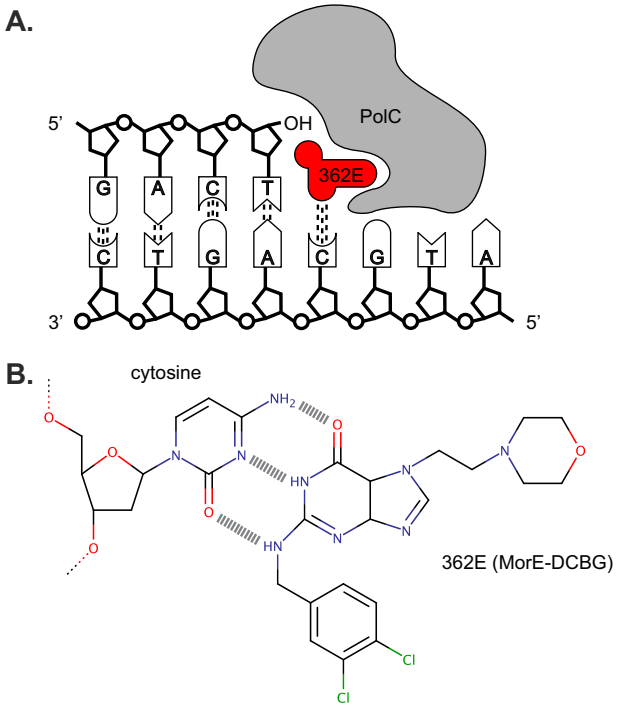

FIG 1 Mechanism of action of the PolC inhibitors ACX-362E. (A) Ternary complex of inhibitor ACX-362E, DNA, and PolC. (B) H-bonding between inhibitor molecule ACX-362E and a cytosine residue of DNA.

tested for either one of the PolC inhibitors was observed among the clinical isolates tested ($n = 363$). Notably, we observed only a 2-fold difference in MIC_{50} and MIC_{90}, indicating that the compounds have similar activities against nearly all strains. In contrast, the Gram-negative obligate anaerobe *Bacteroides fragilis* was resistant to both polymerase inhibitors under the conditions tested (MIC, >265 μg/ml), as expected for an organism lacking PolC. The Gram-positive bacterium *Staphylococcus aureus*, which was included as a control for the activity of HPUra against this group of bacteria (16, 29), was sensitive to both HPUra and ACX-362E, with MIC values of 2 μg/ml and 1 μg/ml, respectively.

We conclude that ACX-362E is highly active against diverse clinical isolates of *C. difficile*, and resistance is not a concern in currently circulating strains.

Treatment with ACX-362E leads to a pleiotropic transcriptional response. In order to determine the transcriptional response of PolC inhibitors, we established the

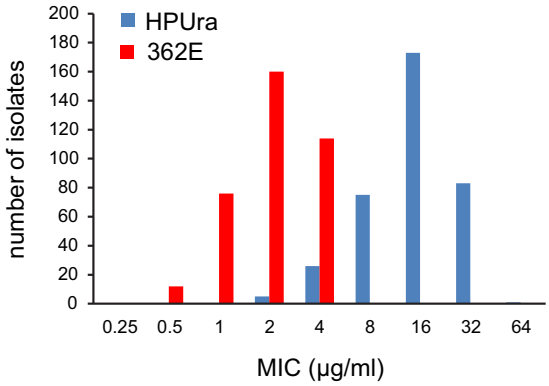

FIG 2 MICs of PolC inhibitors. MIC was determined by agar dilution according to CLSI standards (26) and is expressed in micrograms per milliliter. The distribution in the MIC for the collection of clinical isolates ($n = 363$) is given for the PolC inhibitors HPUra (blue) and ACX-362E (red).

TABLE 1 MICs of PolC inhibitors toward *C. difficile* stratified by clade

Inhibitor by clade	MIC data (μg/ml)			No. of isolates	PCR ribotype(s)
	MIC_{50}	MIC_{90}	Range		
Clade 1					
HPUra	16	32	2–64	230	001, 002, 003, 005, 009, 010, 011, 012, 014, 015, 018, 025, 026, 029, 031, 037, 050, 051, 053, 056, 057, 064, 070, 081, 084, 087, 106, 118
ACX-362E	2	4	0.25–4		
Clade 2					
HPUra	16	32	2–32	24	016, 019, 027, 075, 208
ACX-362E	2	4	0.5–4		
Clade 3					
HPUra	16	32	4–32	7	023
ACX-362E	4	4	1–4		
Clade 4					
HPUra	8	16	2–16	9	017
ACX-362E	2	4	1–4		
Clade 5					
HPUra	16	32	4–32	43	033, 045, 078, 126
ACX-362E	1	2	0.5–4		
Clade 6					
HPUra	4	4	4	1	131
ACX-362E	4	4	4		
Clade unknown					
HPUra	16	32	4–32	49	013, 024, 039, 046, 063, 090, 093, 097, 099, 101, 107, 110, 137, 139, 150, 154, 159, 161, 176, 202, 205, 207, 228, 229, 230, 231, 232, 234
ACX-362E	2	4	0.5–4		

optimal concentration of both inhibitors which affected the growth of *C. difficile* in liquid medium. The laboratory strain *C. difficile* 630Δ*erm* (PCR ribotype 012, multilocus sequence type [MLST] clade 1) (30, 31) was grown in medium with various amounts of HPUra (10 to 40 μg/ml) or ACX-362E (0.25 to 8 μg/ml). We note that concentrations up to the MIC_{90} (as determined by agar dilution) did not lead to a complete growth arrest in liquid medium in the time course of the experiment (Fig. S1). A difference in the MIC values from agar dilution and (micro)broth methods has been observed before (32). The growth kinetics of *C. difficile* under the influence of varied concentrations of HPUra was marginally affected when using concentrations from 10 to 40 μg/ml, at $>$80% of the nontreated culture. Growth kinetics of cultures containing PolC inhibitor ACX-362E at 1 to 8 μg/ml were similar and resulted in 30 to 40% reduced growth compared to that with the nontreated culture. For subsequent experiments, we used concentrations of PolC inhibitors that result in a maximum reduction in growth of 30% compared to that of a nontreated culture (Fig. S1) (HPUra, 35 μg/ml; ACX-362E, 4 μg/ml).

As described above, we established that growth of *C. difficile* is partially inhibited at certain concentrations of PolC inhibitors. Slowing down or stalling of replication forks might lead to a stressed state, as observed for other organisms (22, 23). As nothing is known about the effect of replication inhibition on the physiology of *C. difficile*, we determined the transcriptional response to replication inhibition by sub-MIC levels of PolC inhibitors through strand-specific RNA sequencing (RNA-Seq).

C. difficile 630Δ*erm* was grown for 5 h in medium with HPUra (35 μg/ml) or ACX-362E (4 μg/ml) starting from an optical density at 600 nm (OD_{600}) of 0.05, after which cells were harvested for RNA isolation. Purified RNA was converted to cDNA and used for RNA-Seq, as described in Materials and Methods. For ACX-362E, 722 genes were differentially expressed, of which 438 genes were upregulated and 284 genes were downregulated. The number of differentially expressed genes in HPUra-treated samples was approximately 2-fold lower, at 360, of which 124 genes were upregulated and 236

genes were downregulated. The full list of differentially regulated genes is available in Table S2, and the top 10 upregulated and top 10 downregulated genes are shown in Table 2 (for HPura) and Table 3 (for ACX-362E). Here, we highlight three aspects of the results.

First, we performed a gene set enrichment analysis (GSEA) (33) via the Genome2D web server (http://genome2d.molgenrug.nl/) using the locus tags of the differentially regulated genes (Table S1) as input. Among the genes upregulated by ACX-362E, there is a strong overrepresentation of those involved in translation, ribosomal structure, and ribosomal biogenesis. Not unexpectedly, replication, recombination, and repair processes are also affected. This suggests that genes from these pathways show a coordinated response in the presence of ACX-362E. Among the genes downregulated in the presence of ACX-362E, the levels of significance for specific processes are generally much lower, suggesting that there is a more heterogeneous response among genes from the same pathway. Nevertheless, metabolic pathways (especially carbon metabolism and coenzyme A transfer) and tellurite resistance were found to be significantly affected. Strikingly, a GSEA on lists of genes that are differentially expressed in the presence of HPUra revealed similar processes to be affected.

The findings from the GSEA prompted us to evaluate the overlap in the lists of differentially regulated genes between the ACX-362E and HPUra data sets in more detail. If the two compounds act via a similar mechanism, we expect a conserved response. Indeed, we observe that >90% of the genes that are upregulated in the presence of HPUra compared to the nontreated condition are also identified as upregulated in the presence of ACX-362E (Fig. 3A). Though the overlap is not as strong for the downregulated genes, we find that >30% of the genes affected by HPUra are also identified as affected by ACX-362E (Fig. 3B). Notably, the directionality of the response is conserved, as no genes were found to be upregulated under one condition but downregulated under the other condition. Based on these observations, we believe that the differentially expressed genes identified in this study are representative for a typical response to inhibition of PolC in *C. difficile*.

Finally, we related the changes in transcription to genome location. *C. difficile* has a single circular chromosome and one origin of replication (*oriC*) from which the process of DNA replication occurs bidirectionally toward the terminus (*terC*) (Fig. 4A). Though neither *oriC* nor *terC* has been definitively defined for *C. difficile*, it is assumed that *oriC* is located at or near *dnaA* (CD0001; CD630DERM_RS00005). The terminal region is generally located at the inflection point of a GC skew ([G−C]/[G+C]) plot. Such a plot places the *terC* region around 2.2 Mb from CD0001, near the CD1931 (CD630DERM_RS10465) open reading frame (Fig. 4A) (34). We noted that the differential expression appeared to correlate with genome location (Tables 2, 3, and S2), as many of the upregulated genes have either low or high gene identifiers (CD numbers) indicative of an origin proximal location; conversely, many of the downregulated genes appear to be located away from *oriC*. Though this correlation is not absolute, we observed a clear trend when plotting the mean fold change against the genome location for all genes (Fig. 4B).

Overall, our data show that inhibition of DNA replication by PolC inhibitors causes a consistent and pleiotropic transcriptional response that is at least in part is directly dictated by genome location.

Gene dosage shift occurs at subinhibitory concentration of ACX-362E PolC inhibitor. A possible explanation for the relative upregulation of *oriC*-proximal genes and downregulation of *terC*-proximal genes is a gene dosage shift (35–37), due to the fact that PolC inhibition slows replication elongation but does not prevent reinitiation of DNA replication (23, 38). To determine if this in fact occurs in *C. difficile* when replication elongation is inhibited, we performed a marker frequency analysis (MFA) to determine the relative abundance of an origin-proximal gene relative to a terminus-proximal gene on chromosomal DNA isolated from treated and nontreated cells.

We designed quantitative PCR (qPCR) probes against the CD0001 and CD1931 regions, representing *oriC* and *terC*, respectively (31, 34). Using these probes, we could

TABLE 2 Genes most highly up- and downregulated in the presence of HPUra compared to nontreated cells[d]

RefSeq locus tag by gene group[a]	log(FC)	log(CPM)	LR	*t* test *P* value	Adjusted *P* value	Fold change	minFDR	Old locus tag[b]	Gene name[c]	Product	RefSeq accession no.
Top 10 most significantly upregulated genes											
CD630DERM_RS12480	11.16	3.84	9.8	1.8e−03	2.4e−02	2,291.8	5.37	CD630DERM_23052	CD2305B	Hypothetical protein	WP_004454601.1
CD630DERM_RS15730	6.02	12.24	39.2	3.9e−10	1.9e−07	64.9	22.30			Hypothetical protein	WP_032506906.1
CD630DERM_RS17185	5.12	8.69	48.8	2.9e−12	3.8e−09	34.8	27.97	CD630DERM_32060	CD3206	Hypothetical protein	WP_003434302.1
CD630DERM_RS17015	4.64	8.61	45.7	1.3e−11	1.0e−08	25.0	26.55	CD630DERM_31740	CD3174	Type I glyceraldehyde-3-phosphate dehydrogenase	WP_003421962.1
CD630DERM_RS17020	4.62	8.68	54.7	1.4e−13	2.7e−10	24.6	31.77	CD630DERM_31750	CD3175	Transcriptional regulator	WP_003429564.1
CD630DERM_RS00700	4.37	10.08	33.9	5.8e−09	2.1e−06	20.7	18.85	CD630DERM_00801	CD0080A	50S ribosomal protein L29	WP_003421158.1
CD630DERM_RS00655	4.26	8.55	22.7	1.9e−06	1.4e−04	19.1	12.77	CD630DERM_00720	CD0072	30S ribosomal protein S10	WP_011860633.1
CD630DERM_RS16270	3.96	8.16	34.9	3.5e−09	1.4e−06	15.6	19.44	CD630DERM_30310	CD3031	Transcriptional antiterminator	WP_003432034.1
CD630DERM_RS19860	3.93	10.72	31.8	1.7e−08	4.1e−06	15.2	17.89	CD630DERM_36630	CD3663	30S ribosomal protein S6	WP_003420522.1
CD630DERM_RS00775	3.83	6.09	15.1	1.0e−04	2.7e−03	14.2	8.53	CD630DERM_00930	CD0093	50S ribosomal protein L14	WP_009895197.1
Top 10 most significantly downregulated genes											
CD630DERM_RS09945	−14.85	4.52	17.0	3.7e−05	1.2e−03	−29,514.0	9.72	CD630DERM_17940	CD1794	Hypothetical protein	WP_003430297.1
CD630DERM_RS12730	−14.52	4.33	17.3	3.1e−05	1.1e−03	−23,428.2	9.87	CD630DERM_23550	CD2355	Thiol reductase thioredoxin	WP_003416870.1
CD630DERM_RS00870	−14.39	4.91	21.8	3.0e−06	1.9e−04	−21,483.7	12.35			tRNA-Asn	
CD630DERM_RS00255	−14.35	5.48	45.8	1.3e−11	1.0e−08	−20,874.2	26.55			tRNA-His	
CD630DERM_RS00925	−14.18	4.91	23.1	1.5e−06	1.3e−04	−18,514.8	12.89			tRNA-Ser	
CD630DERM_RS17905	−14.02	5.11	26.3	3.0e−07	4.1e−05	−16,646.0	14.57			Hypothetical protein	WP_042741280.1
CD630DERM_RS05300	−14.01	4.27	12.7	3.7e−04	7.3e−03	−16,475.8	7.11	CD630DERM_09230	CD0923	Hypothetical protein, putative phage protein	WP_021362052.1
CD630DERM_RS00170	−13.98	4.82	13.8	2.0e−04	4.5e−03	−16,156.5	7.78			tRNA-Asn	
CD630DERM_RS03115	−13.96	5.24	56.8	4.8e−14	1.9e−10	−15,908.4	32.28	CD630DERM_04981	CD0498A	Hypothetical protein	WP_011860839.1
CD630DERM_RS05160	−13.92	3.89	15.3	9.1e−05	2.5e−03	−15,523.8	8.65	CD630DERM_08960	CD0896	Hypothetical protein	WP_003418667.1

[a]At time of analysis: https://www.ncbi.nlm.nih.gov/nuccore/NZ_LN614756.1.
[b]https://www.ncbi.nlm.nih.gov/nuccore/LN614756.1.
[c]https://www.ncbi.nlm.nih.gov/nuccore/AM180355.1.
[d]log(FC), log2 fold change; log(CPM), log2 counts per million; LR, likelihood ratio; adjusted *P* value, Benjamini Hochberg corrected *P* value; minFDR, −log2(adj-pvalue).

TABLE 3 Genes most highly up- and downregulated in the presence of ACX-362E compared to nontreated cells[d]

RefSeq locus tag by gene group[a]	log(FC)	log(CPM)	LR	*t* test *P* value	Adjusted *P* value	Fold change	minFDR	Old locus tag[b]	Gene name[c]	Product	RefSeq accession no.
Top 10 most significantly upregulated genes											
CD630DERM_RS12480	11.31	3.84	9.9	1.6e−03	1.3e−02	2,544.2	6.25	CD630DERM_23052	CD2305B	Hypothetical protein	WP_004454601.1
CD630DERM_RS17185	7.73	8.69	87.6	8.1e−21	3.3e−17	211.9	54.77	CD630DERM_32060	CD3206	Hypothetical protein	WP_003434302.1
CD630DERM_RS17955	6.88	7.78	28.5	9.5e−08	5.0e−06	117.8	17.62	CD630DERM_33520	CD3352	AraC family transcriptional regulator	WP_009891821.1
CD630DERM_RS17950	6.87	9.82	31.9	1.6e−08	1.0e−06	117.3	19.88	CD630DERM_33510	CD3351	ATP-dependent Clp protease proteolytic subunit	WP_003436212.1
CD630DERM_RS15730	6.67	12.24	45.3	1.7e−11	4.0e−09	101.9	27.89			Hypothetical protein	WP_032506906.1
CD630DERM_RS00990	5.92	8.75	50.1	1.4e−12	5.7e−10	60.4	30.70	CD630DERM_01090	CD0109	Anaerobic ribonucleoside-triphosphate reductase activating protein	WP_003432598.1
CD630DERM_RS00655	5.65	8.55	35.0	3.2e−09	2.7e−07	50.3	21.80	CD630DERM_00720	CD0072	30S ribosomal protein S10	WP_011860633.1
CD630DERM_RS00985	5.50	8.94	66.3	3.8e−16	7.6e−13	45.2	40.27	CD630DERM_01080	CD0108	Anaerobic ribonucleoside triphosphate reductase	WP_003436320.1
CD630DERM_RS05405	5.49	10.12	43.5	4.2e−11	8.0e−09	45.0	26.89	CD630DERM_09410	CD0941	Hypothetical protein	WP_009894743.1
CD630DERM_RS15695	5.24	10.08	41.5	1.2e−10	2.0e−08	37.9	25.61	CD630DERM_29250	CD2925	Hypothetical protein	WP_009894743.1
Top 10 most significantly downregulated genes											
CD630DERM_RS05350	−14.17	5.04	40.4	2.1e−10	3.1e−08	−18,382.7	24.94	CD630DERM_09310	CD0931	Hypothetical protein	WP_011861014.1
CD630DERM_RS05160	−13.92	3.89	15.0	1.1e−04	1.6e−03	−15,523.8	9.33	CD630DERM_08960	CD0896	Hypothetical protein	WP_003418667.1
CD630DERM_RS05375	−13.72	4.09	14.3	1.5e−04	2.0e−03	−13,454.4	8.95	CD630DERM_09360	CD0936	Endonuclease	WP_011861020.1
CD630DERM_RS15535	−13.57	4.30	23.5	1.3e−06	4.4e−05	−12,181.6	14.47	CD630DERM_28950	CD2895	Membrane protein	WP_011861046.1
CD630DERM_RS13040	−13.55	3.91	11.4	7.5e−04	7.1e−03	−11,987.2	7.15	CD630DERM_24140	CD2414	PTS sorbose transporter subunit IIB	WP_003430855.1
CD630DERM_RS05345	−13.55	4.41	16.5	4.9e−05	8.2e−04	−11,969.7	10.25	CD630DERM_09301	CD0930A	Hypothetical protein	WP_011861013.1
CD630DERM_RS11925	−13.53	4.10	14.0	1.9e−04	2.3e−03	−11,799.9	8.76	CD630DERM_21991	CD2199A	4Fe-4S ferredoxin	WP_003423406.1
CD630DERM_RS01060	−13.52	4.51	14.9	1.1e−04	1.6e−03	−11,718.7	9.33			tRNA-Glu	
CD630DERM_RS15350	−13.44	3.89	15.3	9.1e−05	1.4e−03	−11,076.8	9.53			Membrane protein	WP_003426729.1
CD630DERM_RS06360	−13.43	4.12	23.9	1.0e−06	3.7e−05	−11,012.2	14.72	CD630DERM_11160	CD1116	Transposase	WP_011861118.1

[a]At time of analysis: https://www.ncbi.nlm.nih.gov/nuccore/NZ_LN614756.1.
[b]https://www.ncbi.nlm.nih.gov/nuccore/LN614756.1.
[c]https://www.ncbi.nlm.nih.gov/nuccore/AM180355.1.
[d]PTS, phosphotransferase system; log(FC), log2 fold change; log(CPM), log2 counts per million; LR, likelihood ratio; adjusted *P* value, Benjamini Hochberg corrected *P* value; minFDR, −log2(adj-pvalue).

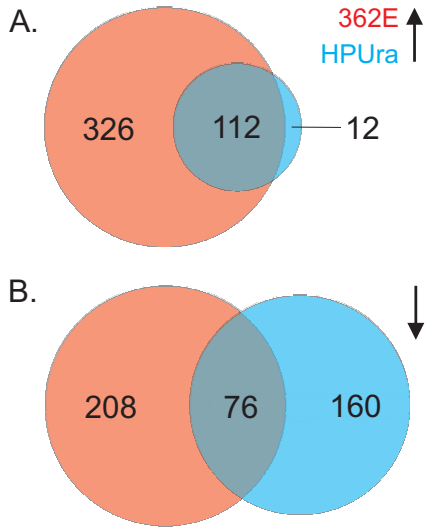

FIG 3 Overlap in the transcriptional response to different PolC inhibitors. (A) Venn diagram of the number of genes upregulated in the presence of ACX-362E (red), in the presence of HPUra (blue), or under both conditions (overlapping region). (B) Venn diagram of the number of genes downregulated in the presence of ACX-362E (red), in the presence of HPUra (blue), or under both conditions (overlapping region). The sizes of the circles are proportional to the number of genes that showed differential expression.

show that *C. difficile* demonstrates multifork replication in exponential-growth phase and that the MFA assay detects the expected decrease in *oriC*/*terC* ratio when cells enter stationary-growth phase (data not shown). Next, we analyzed the effects of PolC inhibitors on the *oriC*/*terC* ratio. When cells were treated with HPUra (35 μg/ml), the MFA showed a modest increase in *oriC*/*terC* ratio of 2.6-fold compared to nontreated cells. However, when cells were treated with ACX-362E (4 μg/ml), the MFA showed a >8-fold increase in the *oriC*/*terC* ratio compared to nontreated cells. In contrast, such an increase was not observed for cells treated with 0.25 μg/ml metronidazole (a DNA-damaging agent), 0.00125 μg/ml fidaxomicin (an RNA polymerase inhibitor),

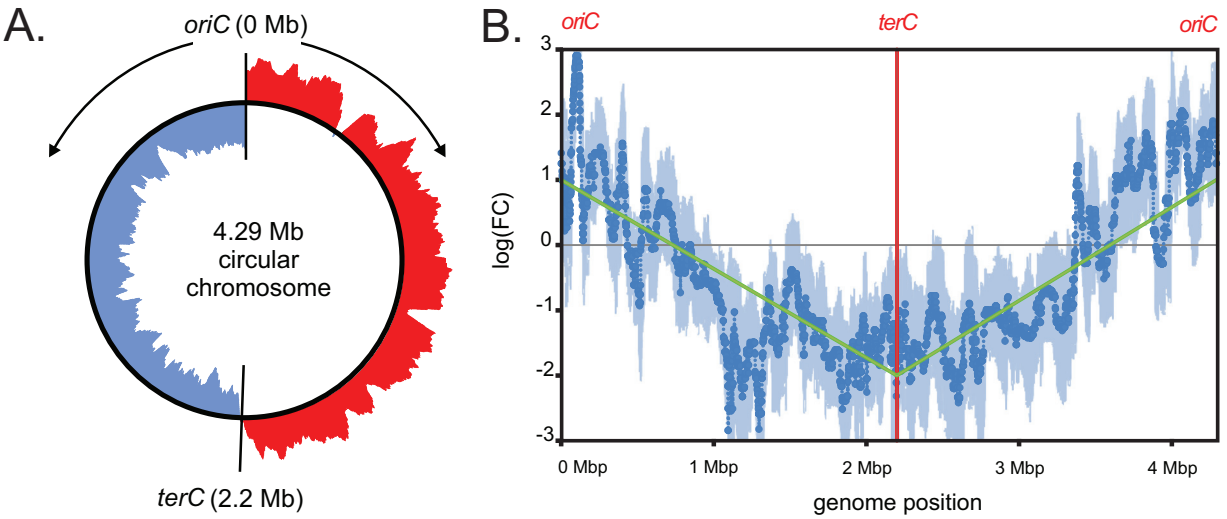

FIG 4 Genome location correlates with differential expression upon PolC inhibition. (A) Schematic representation of the chromosome of *C. difficile*. Higher-than-average GC skew ([G−C]/[G+C]) (red) and lower-than-average GC skew (blue) were calculated with DNAPlotter (https://www.sanger.ac.uk/science/tools/dnaplotter). Vertical lines indicate the position of the predicted origin (*oriC*) and terminus (*terC*) of replication. Arrows indicate the direction of replication. (B) Sliding window analysis (bins of 51 loci; step size, 1) of the median log fold change (FC) projected on a linear genome map. The *oriC* of the circular chromosome is located on either size of the linear graph (0/4.29 Mb), whereas *terC* is indicated with a vertical red line. The trend in log(FC) is highlighted using a green line. Light-blue shading indicates the median absolute deviation of the mean (23).

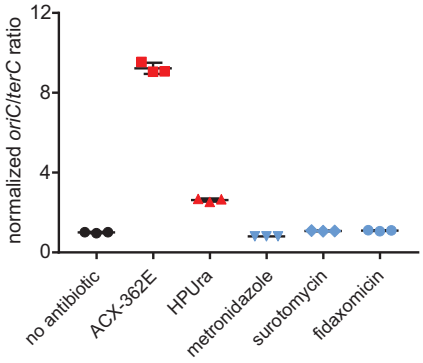

FIG 5 Polymerase inhibitors lead to an increase in *oriC*/*terC* ratio. A marker frequency analysis of the effects of subinhibitory amounts of polymerase inhibitors (red; HPUra, 35 μg/ml; ACX-362E, 4 μg/ml) and three antibiotics with different modes of action (blue; metronidazole, 0.25 μg/ml; fidaxomicin, 0.00125 μg/ml, surotomycin, 0.625 μg/ml) compared to nontreated cells (black). Data points are averages of technical replicates ($n = 3$). Black lines behind the data points indicate the average of the biological replicates ($n = 3$), and whiskers indicate the standard deviation of the mean. Data have been normalized compared to the nontreated control. The mean of HPUra- and ACX-362E-treated samples is statistically different from the other samples ($P < 0.0001$).

0.625 μg/ml surotomycin (a cell wall synthesis inhibitor) (Fig. 5), or 2 μg/ml chloramphenicol (a protein synthesis inhibitor) (Fig. S2).

We conclude that the inhibition of PolC activity, but not the actions of any of the other tested antimicrobials, leads to a gene dosage shift in *C. difficile*.

Origin-proximal *sigB* contributes to the transcriptional response. Elegant work in *S. pneumoniae* has shown that the transcriptional response to replication inhibition can also be affected by origin-proximal regulators that respond to the gene dosage effect (23). In *C. difficile*, the gene encoding the general stress response sigma factor σ^B (*sigB*, CD0011) is located close to the origin of replication (39). We wondered whether this regulator contributes to the transcriptional effects observed in our studies.

First, we compared the list of differentially regulated genes from our study (Table S2) to those under the control of σ^B (40). In contrast to most anaerobic Gram-positive organisms, *C. difficile* encodes a homolog of the general stress response sigma factor σ^B (39, 41). A transcriptome analysis comparing a *sigB* mutant versus wild-type cells was recently published (40). Strikingly, we found ~40% of the genes (21/58) identified as involved in stress response under the control of σ^B to be differentially expressed in our ACX-362E data set (Table S3). Similarly, we observed that 7/20 (~35%) of the genes containing a transcriptional start site with a σ^B consensus sequence are differentially expressed in our ACX-362E data set (Table S3). These data suggest that the response to DNA replication inhibition is at least partially dependent on σ^B.

To demonstrate that exposure to ACX-362E causes a transient upregulation of *sigB*, we constructed a reporter fusion of the secreted luciferase reporter sLuc^{opt} with the predicted promoter of the *sigB* operon (P_{cd0007}). We monitored the luciferase activity of a strain harboring a plasmid containing this reporter fusion (WKS2003) after dilution of an overnight culture into fresh medium with or without ACX-362E (Fig. 6). In nontreated cells, expression from the *sigB* promoter is relatively stable over the course of 5.5 h. In contrast, luciferase activity strongly increases from 1.25 h to 3 h after inoculation into medium with ACX-362E. These data show that exposure to ACX-362E transiently induces transcription of the *sigB* operon.

Next, a *sigB* mutant was constructed using allele-coupled exchange (42), as described in Materials and Methods. The chromosomal deletion of *sigB* and absence of the σ^B protein were verified by PCR and Western blotting, respectively (Fig. S3). To directly demonstrate a role for *sigB* in the regulation of genes with altered transcription upon PolC inhibition, we fused the predicted promoter regions of selected genes to a secreted luciferase reporter (43) and evaluated luminescence in wild-type and *sigB* mutant backgrounds after 5 h of growth in the presence and absence of 4 μg/ml

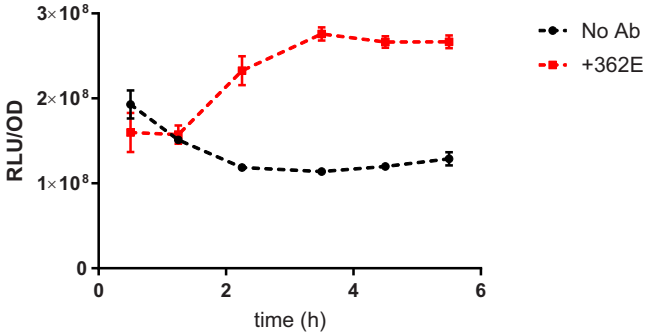

FIG 6 The *sigB* operon is transiently induced upon exposure to ACX-362E. The putative promoter of the *sigB* operon (40) was fused transcriptionally to a plasmid-based luciferase reporter (43). Luciferase activity was measured regularly between 30 min and 5.5 h of growth in liquid medium in the presence (+362E) or absence (no antibody [Ab]) of polymerase inhibitor ACX-362E. RLU, relative light units.

ACX-362E. All genes tested demonstrated a significant increase in promoter activity in a wild-type background in the presence of ACX-362E compared to the nontreated control, validating the results from the RNA-Seq analysis (Fig. 7). Three distinct patterns were observed. For CD0350 (encoding a hypothetical protein) and CD2963 (encoding a putative peptidoglycan-binding exported protein), there was virtually no expression in a *sigB* mutant background (Fig. 7A and B). We conclude that these genes are strictly dependent on σ^B for their expression under the conditions tested. CD3614 (encoding a hypothetical protein) shows a basal level of expression but no significant increase in transcription levels in the presence of ACX-362E in a *sigB* mutant background com-

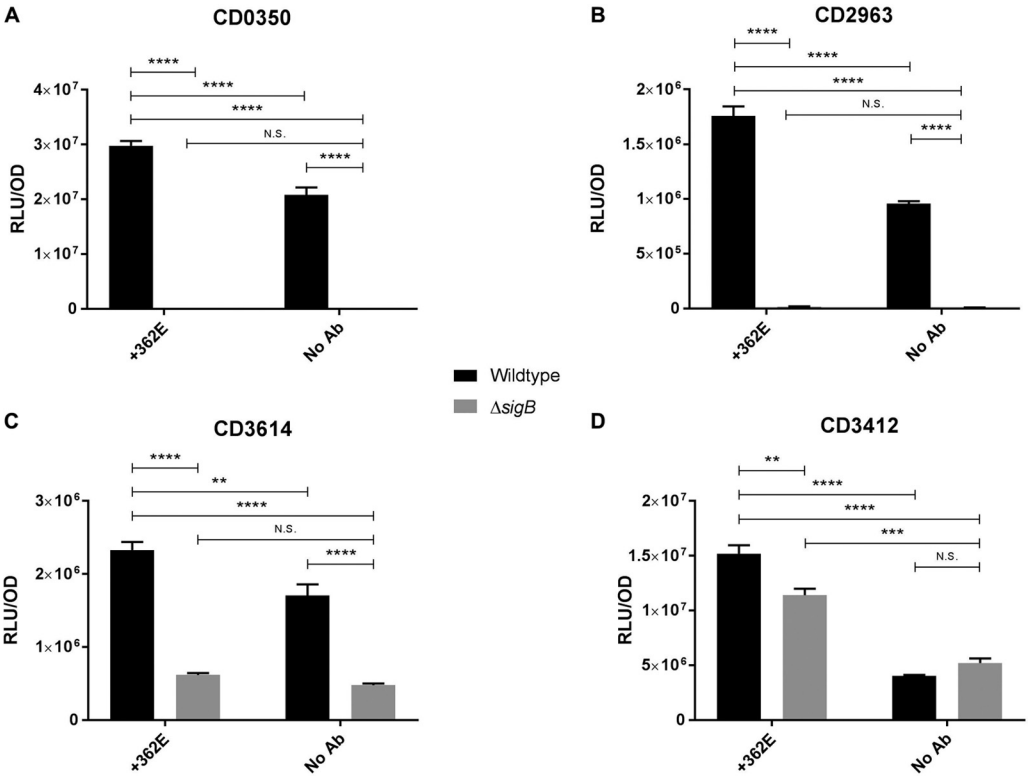

FIG 7 Genes differentially expressed due to polymerase inhibitors are regulated by σ^B. The putative promoters of the indicated genes were fused transcriptionally to a plasmid-based luciferase reporter (43). Luciferase activity was measured after 5 h of growth in liquid medium in the presence (+362E) or absence (no Ab) of polymerase inhibitor ACX-362E. N.S., nonsignificant; *, $P < 0.05$; **, $P < 0.005$; ***, $P < 0.0005$; ****, $P < 0.00005$. (A) P_{CD350}-*sLuc*^{opt}. (B) P_{CD2963}-*sLuc*^{opt}. (C) P_{CD3614}-*sLuc*^{opt}. (D) P_{CD3412}-*sLuc*^{opt}.

pared to the nontreated control (Fig. 6C). This suggests that the transcriptional upregulation under these conditions is σ^B dependent, and it indicates that the basal level of transcription observed is likely independent of σ^B. Finally, CD3412 (*uvrB*, encoding a subunit of an excinuclease) shows reduced transcriptional upregulation in ACX-362E-treated cells compared to the nontreated controls (Fig. 6D). Thus, the transcription of this particular gene under conditions of ACX-362E exposure is brought about by both σ^B-dependent and σ^B-independent regulatory pathways.

Together, these results demonstrate that *sigB* controls the expression of at least a subset of genes that are upregulated under PolC inhibition.

DISCUSSION

Activity and specificity of ACX-362E. Limited treatment options and reports of reduced susceptibility to current treatment (11, 12, 44) emphasize the necessity for the development of novel antimicrobials. As CDI can be induced by the use of broad-spectrum antibiotics (7), new antimicrobials ideally should only target *C. difficile*, thereby maintaining the integrity of the colonic microbiota. In this study, we have tested the inhibitors HPUra and ACX-362E that specifically target the PolC enzyme, which is essential for DNA replication. The majority of PolC inhibitors target Gram-positive bacteria with low G+C content, but ACX-362E has been reported to demonstrate increased specificity toward *C. difficile* PolC *in vitro* and showed promising results for efficacy *in vivo* based on a limited set of *C. difficile* strains (19, 20). The compound will progress to clinical trials in the near future (Acurx Pharmaceuticals, personal communication). The present study is the largest survey of the efficacy of HPUra and ACX-362E against a large collection of clinical isolates consisting of many relevant PCR ribotypes to date. We have established that ACX-362E demonstrated lower inhibitory concentrations than the general Gram-positive PolC inhibitor HPUra in agar dilution experiments. The MIC_{50} and MIC_{90} of ACX-362E are similar to those of antimicrobials commonly used to treat *C. difficile* infection (for metronidazole, MIC_{50}, 2 μg/ml, and MIC_{90}, 4 μg/ml; for vancomycin, MIC_{50}, 2 μg/ml, and MIC_{90}, 4 μg/ml [20]; for fidaxomicin, MIC_{50}, 0.125 μg/ml, and MIC_{90}, 0.5 μg/ml [45]). We did not detect a significant difference in MICs between clades and ribotypes, demonstrating that PolC inhibitors have the potential to be used as treatment for the majority of, if not all, circulating *C. difficile* strains. This includes the epidemic types of PCR ribotypes 027 and 078 (8, 46). These results are in line with other work that demonstrated only 2- to 4-fold differences in antimicrobial susceptibility between different clades for metronidazole, fidaxomicin, and semisynthetic thiopeptide antibiotic LFF571 (28). In the course of our experiments, we did not find any strains that grew at the highest concentrations of either HPUra or ACX-362E tested. PolC inhibitors are competitive inhibitors of polymerase activity by binding in the active site. Mutations that abolish binding of HPUra or ACX-362E are likely to affect the essential enzymatic activity of the polymerase and for that reason are unlikely to occur *in vivo*. A single mutation (*azp-12*) has been described in *B. subtilis* that confers resistance to HPUra (47). This T-to-G transversion results in the replacement of a serine with an alanine in the highly conserved PFAM07733 domain of the polymerase (48). To our knowledge, it is unknown whether this mutation prevents binding of HPUra to PolC of *B. subtilis*. Few other mutations have been described that confer resistance against other PolC inhibitors (49, 50). It will be of interest to see if similar mutations in *C. difficile* result in resistance to HPUra and/or ACX-362E and what the effect is on binding of these compounds to *C. difficile* PolC.

ACX362 may have off-target effects unrelated to its replication-inhibitory activity. For *C. difficile*, it has not been established that PolC inhibition is the sole mode of action of the inhibitors. In our experiments, we found that *S. aureus* was sensitive to both HPUra and ACX-362E and even more so than *C. difficile*. It should be established if this is due to inhibition of PolC or is mediated by an alternative mechanism. If ACX-362E targets DNA replication in *S. aureus*, we would also expect to find an increase in the *oriC*/*terC* ratio upon ACX-362E exposure in this organism. Alternatively, ACX-362E may also affect the activity of the other PolIII-type polymerase DnaE in *S. aureus*. PolIII

inhibitors can affect PolC, DnaE, or both (50), though *in vivo* activity appears to correlate with PolC inhibition. Both *C. difficile* and *S. aureus* possess PolC and DnaE polymerase, but the DnaE enzymes are of different families (DnaE1 in *C. difficile* and DnaE3 in *S. aureus*) (51). To verify the mode of action, and whether different DnaE-type polymerases explain the increased sensitivity of *S. aureus* compared to *C. difficile*, the activity of ACX-362E toward purified DnaE and PolC from both organisms should be determined.

Though it is clear that ACX-362E inhibits *C. difficile* efficiently and shows limited activity toward certain other anaerobes (19), these findings highlight the necessity to perform additional (microbiome) studies to more clearly define the antimicrobial spectrum of this compound. It also shows that ACX-362E may have therapeutic potential outside treatment for CDI.

Regulators of the transcriptional response to PolC inhibitors. The present study is the first to describe the transcriptional response of *C. difficile* to inhibition of DNA replication. We find that ~200 genes show differential expression under conditions of PolC inhibition by both HPUra and ACX-362E compared to nontreated cells. When considering only ACX-362E, approximately 13% of all genes in the genome show statistically significant altered transcription. We demonstrate that this large reprogramming of transcription is likely to be caused directly by a gene dosage shift.

In addition to direct effects, it is conceivable that at least part of the transcriptional response is indirect. Our list of differentially regulated genes includes several putative regulators, as follows: sigma factors (including *sigE*, *sigG*, and *sigH*), transcription factors, and antiterminators. The relatively long time (5 h) at sub-MIC levels of antimicrobials may have contributed to secondary effects through one or more of these regulators. Though shorter induction times are thought to provoke more compound-specific responses (52), we did observed a highly consistent transcriptional signature with both HPUra and ACX-362E.

Major stress response pathways are poorly characterized in *C. difficile*. On the basis of experiments in other organisms (21–23, 53–55), we expect that the inhibition of DNA replication inhibition might possibly induce an SOS response (LexA) (56), a DnaA-dependent transcriptional response (21), and possibly a heat shock response (HrcA/CtsR) (57) and/or a general stress response (σ^B) (41). Of these, the best characterized stress response pathway in *C. difficile* is the one governed by σ^B (40). We noted a significant overlap in putatively σ^B-dependent genes and those differentially expressed upon exposure to PolC inhibitors. In addition, our luciferase reporter fusions directly implicate *sigB* in the expression and/or upregulation of some of these. It should be noted that the *sigB* operon itself was not differentially expressed in our RNA-Seq analysis. A *sigB*-reporter fusion suggests that *sigB* is transiently upregulated prior to the time point of sampling for the RNA-Seq analysis. Similar transient upregulation of *sigB* followed by a persistent response of σ^B-dependent gene expression has been observed in other organisms (57–59). To our knowledge, this is the first indication that *sigB*- and SigB-dependent gene expression could be subject to a gene dosage effect.

To date, no genes have been identified that are regulated by DnaA in *C. difficile*, and direct regulation of genes through the other stress response pathways has not been demonstrated. Many parameters (such as the medium used, cell density, concentration of antibiotics, and protocol used to arrest transcription between cell harvest and lysis) can influence overall transcription signatures (52) and can also govern an incomplete overlap between our data and the stress regulons proposed by others (58–60).

Genome location contributes to the transcriptional response to PolC inhibition. Our analysis of differential regulation in relation to genome location revealed a striking pattern of relative upregulation for *oriC*-proximal genes and downregulation for *terC*-proximal genes under conditions of PolC inhibition. Antimicrobials directed at DNA replication in bacteria have a profound negative effect on the processivity of replication forks, though initiation of DNA replication is not or is only marginally affected (23, 38). As a consequence, the presence of multiple replication forks simul-

taneously increases the copy numbers of genes located in close proximity of the origin of replication, and such a gene dosage differences can result in functionally relevant transcriptional differences, either directly or indirectly (15). We found an increase of *oriC*/*terC* ratio when performing MFA on chromosomal DNA of cells subjected to a subinhibitory concentration of ACX-362E (and HPUra, albeit less pronounced), consistent with findings in other organisms (23). This is the first demonstration of gene dosage-dependent transcriptional regulation in *C. difficile*. Our experiments suggest that at least part of the transcriptional response to PolC inhibition can be explained by an indirect gene dosage effect, as also observed for *S. pneumoniae* (23). The positioning of stress response regulators close to *oriC* may therefore be a conserved strategy in bacteria to respond to DNA replication insults, independent of the nature of the regulator.

Though it is likely that an increase in gene copy number leads to an increase in the transcription of these genes, it is less clear whether this is the case for the observed downregulation. Most methods of normalization for transcriptome analyses are based on the assumption that there is no overall change in transcription or that the number of transcripts per cells is the same for all conditions; this may not be the case when a global copy number shift occurs (15). Absolute transcript levels for downregulated genes might therefore be similar under the two conditions (but lower than *oriC*-proximal transcripts).

It is interesting that certain processes are highly enriched in the list of genes upregulated under conditions of PolC inhibition (most notably ribosome function and DNA-related functions), whereas this is less so for the downregulated genes. This suggests that pathways susceptible to replication-dependent gene dosage effects demonstrate a functional clustering of genes near *oriC*, whereas clustering of genes from specific pathways in the *terC*-proximal region is less pronounced. Indeed, most ribosomal gene clusters in *C. difficile* are located close to the origin of replication (31, 39), and many genes involved in DNA replication and repair are located in these regions. Consistent with this, the positioning of genes involved in transcription and translation close to the origin appears to be under strong selection, as such genomes tend to be more stable (61).

In conclusion, both direct and indirect effects of gene dosage shifts are likely to contribute to the transcriptional response of *C. difficile* to replication inhibition.

MATERIALS AND METHODS

Bacterial strains and culture conditions. Plasmids and bacterial strains used in this study can be found in Table 4 (note that this table only contains laboratory strains; the clinical isolates used for the agar dilution experiments [see below] are listed in Table S1). *E. coli* was cultured aerobically at 37°C (shaking at 200 rpm) in Luria-Bertani (LB) broth supplemented with 20 μg/ml chloramphenicol and 50 μg/ml kanamycin when appropriate. *C. difficile* strains were cultured in brain heart infusion (BHI) broth (Oxoid) supplemented with 0.5% yeast extract (Sigma-Aldrich), *Clostridium difficile* selective supplement (CDSS; Oxoid), and 20 μg/ml thiamphenicol when appropriate. *C. difficile* was grown anaerobically in a Don Whitley VA-1000 workstation in an atmosphere of 10% CO_2, 10% H_2, and 80% N_2. Liquid cultures were grown under gentle agitation (120 rpm).

Agar dilution. HPUra and ACX-362E were tested against a collection of *C. difficile* clinical isolates. Three hundred seventy-five clinical isolates have been collected during the ECDIS study (6). All strains were characterized by PCR ribotyping (62) and by PCR to confirm the presence of genes encoding toxins A and B and binary toxin (63–65). Of the 375 clinical isolates, we excluded stocks that were found to contain more than one strain and isolates that could not be recultured. Testing was therefore performed on 363 isolates (Table S1). *C. difficile* ATCC 700057, *B. fragilis* ATCC 25285, and *S. aureus* ATCC 29213 were used as controls (ATCC).

The strains were tested for the different concentrations of antimicrobial using the agar dilution method, according to Clinical and Laboratory Standards Institute guidelines (26, 27). In short, the antimicrobials were diluted into brucella blood agar (BBA) supplemented with hemin and vitamin K_1. Bacterial isolates were cultured on blood agar plates and after 24 h resuspended to a turbidity of 0.5 McFarland in phosphate-buffered saline (PBS). The strains were inoculated onto BBA solid medium containing the PolC inhibitors using multipoint inoculators to a final concentration of 10^4 CFU per spot. Each series of antimicrobial agents was tested from the lowest concentration to the highest concentration. Two control plates without antibiotics were inoculated to control for aerobic contamination and purity of anaerobic growth. At the end of the final series, two control plates were inoculated to verify the final organism viability and purity. Only experiments where both positive and negative controls per-

TABLE 4 Plasmids and strains used in this study

Plasmid or strain	Relevant features[a]	Source/reference
Plasmids		
pAP24	*tetR* P*tet-sluc*^{opt} *catP*; derived from pRPF185	43
pIB27	P_{CD3412}-*sluc*^{opt} *catP*; derived from pAP24	This study
pIB54	pMTL-SC7315 containing the up- and downstream area of the 630Δ*erm* σ^B CDS (950 bp each)	This study
pIB68	P_{CD0350}-*sluc*^{opt} *catP*; derived from pAP24	This study
pIB69	P_{CD2963}-*sluc*^{opt} *catP*; derived from pAP24	This study
pIB74	P_{CD3614}-*sluc*^{opt} *catP*; derived from pAP24	This study
pMTL-SC7315	pMTL83151 with *codA catP*	42
pH28	P_{CD0007}-*sluc*^{opt} *catP*; derived from pAP24	This study
Strains		
Escherichia coli		
DH5α	F$^-$ *endA1 glnV44 thi-1 recA1 relA1 gyrA96 deoR nupG purB20 φ80dlacZ*ΔM15 Δ(*lacZYA-argF*)*U169 hsdR17*(r_K^- m_K^+) λ^-	Laboratory stock
CA434	HB101 [F$^-$ *mcrB mrr hsdS20*(r_B^- m_B^-) *recA14 leuB6 ara-14 proA2 lacY1 galK2 xyl-5 mtl-1 rspL20(SmR)glnV44* λ^-] R702	68
C. difficile 630Δ*erm*	MLS-susceptible derivative of strain 630	30, 31
IB37	630Δ*erm*/pIB27; thia^r	This study
IB56	630Δ*erm* Δ*sigB*	This study
IB95	630Δ*erm*/pIB68; thia^r	This study
IB96	630Δ*erm*/pIB69; thia^r	This study
IB98	IB56/pIB27; thia^r	This study
IB99	IB56/pIB68; thia^r	This study
IB100	IB56/pIB69; thia^r	This study
IB108	630Δ*erm*/pIB74; thia^r	This study
IB111	IB54/pIB74; thia^r	This study
WKS2003	630Δ*erm*/pPH28; thia^r	This study

[a]MLS, macrolides-lincosamides-streptogramins; thia^r, thiamphenicol resistance.

formed according to expectations were included. Plates were incubated anaerobically in a Don Whitley VA-1000 workstation in an atmosphere of 10% CO_2, 10% H_2, and 80% N_2, and the MICs were recorded after 24 and 48 h and are presented in this paper with values at 48 h, according to the CLSI guidelines (26).

Sub-MIC determination. *C. difficile* 630Δ*erm* (30, 31) was grown in 20 ml brain heart infusion (Oxoid) supplemented with 0.5% yeast extract (BHI/YE; Sigma-Aldrich) starting from an optical density at 600 nm (OD_{600}) of 0.05 using an exponentially growing starter culture (3 biological replicates per concentration). To determine the effects on growth at subinhibitory concentrations of ACX-362E, cells were cultured in the presence of the concentrations 0.25, 0.5, 1, 2, 4, and 8 μg/ml ACX-362E and compared to an nontreated culture. To determine the effects on growth at subinhibitory concentrations of HPUra, cells were cultured in the presence of the concentrations 10, 20, and 40 μg/ml HPUra and compared to an nontreated culture. The OD_{600} was monitored every hour until stationary phase was reached.

Marker frequency analysis. *C. difficile* 630Δ*erm* (30, 31) was grown in 20 ml BHI supplemented with 0.5% yeast extract with sub-MIC amounts of antimicrobials (HPUra, 35 μg/ml; ACX-362E, 4 μg/ml; metronidazole, 0.25 μg/ml; fidaxomicin, 0.00125 μg/ml, surotomycin, 0.625 μg/ml), starting from an OD_{600} of 0.05 using an exponentially growing starter culture. These samples were taken in the course of an independent, but simultaneously performed, set of experiments for which we obtained surotomycin and fidaxomicin from Cubist Pharmaceuticals. Metronidazole was commercially obtained (Sigma-Aldrich). We confirmed that these concentrations did not lead to a >30% reduction in growth compared to the nontreated cultures (Fig. S1 and data not shown). In parallel, cultures were grown without inhibitors from the same starter culture. All conditions were performed in biological triplicates. Previous experiments have shown that *ori*/*ter* differences are reliably detected >3 h after dilution into fresh medium (23). Therefore, after 5 h, 1 ml cells was harvested (OD_{600}, ~0.5) and stored at −20°C. Isolation of chromosomal DNA was performed the next day with the QIAamp DNA blood minikit (Qiagen), according to the instructions of the manufacturer. Marker frequency analysis (MFA) was performed to assess the relative abundance of origin-proximal genes relative to terminus-proximal genes. As a proxy for *oriC*, a probe was designed that targets the CD0001 region (CD0001-probe-FAM). By using plots of the GC skew ([G−C]/[G+C]) generated using DNAPlotter (https://www.sanger.ac.uk/science/tools/dnaplotter), the approximate location of the terminal region for the *C. difficile* chromosome was determined, and a probe targeting this region (CD1931) was designed (CD-1931-probe-TXR). Probe design was performed with Beacon Designer (Premier Biosoft, Palo Alto CA, USA). Real-time PCRs were performed on a Bio-Rad CFX96 real-time PCR detection system (95°C for 15 min, 39 cycles of 94°C for 30 s, 55°C for 30 s, and 72°C 30 s). The sequences for the primers and probes used are listed in Table 5. For each biological replicate, three technical replicates were performed. Amplification efficiency was determined using standard curves obtained from DNA late-stationary-phase cells of strain 630Δ*erm*, for which an *oriC*/*terC* ratio of 1 was assumed. Reverse transcription-PCR (RT-PCR) results from antibiotic-treated

TABLE 5 Oligonucleotides and probes used in this study

Name	Sequence (5′→3′)[a]	Description
CD-0001- F	GAGACAAGAATTGCTATACTTA	Forward primer CD0001 MFA (*oriC*)
CD-0001- R	CAACCACTCTAGTTAATGC	Reverse primer CD0001 MFA (*oriC*)
CD-0001-probe-FAM	CTCAACTAGAACGTATAGATGTGCCAA	Probe CD0001 MFA (*oriC*)
CD-1931- F	GCAGGAATTTTAGATGAAGA	Forward primer CD1931 MFA (*terC*)
CD-1931- R	GGCTGAAGTCTTATTAAATTTC	Reverse primer CD1931 MFA (*terC*)
CD-1931-probe-TXR	CCTCTTAACTGTAGCAGATTCACCAT	Probe CD1931 MFA (*terC*)
oIB-26	GGAAGGTACCGTTGAATAAAGTATTTATTTTCCATG	Forward primer for pCD3412 containing a KpnI restriction site
oIB-27	GGTAGAGCTCAGTATCACTCCTTTTTTCGAAC	Reverse primer for pCD3412 containing an SacI restriction site
oIB-44	CGTAGAAATACGGTGTTTTTTGTTACCCTACTTATAGTAGCAATT TATTTAGCTAAAAC	Forward primer for region 950 bp upstream of *sigB* CDS
oIB-45	TACTTTTTTTATATTTTTTTAAATATCAACTCCTAAATATTTAGTC	Reverse primer for region 950 bp upstream of *sigB* CDS
oIB-46	GGAGTTGATATTTAAAAAAATATAAAAAAAGTATTGACCTACTG	Forward primer for region 950 bp downstream of *sigB* CDS
oIB-47	GGGATTTTGGTCATGAGATTATCAAAAAGGGGACTACCAGGGT ATCTAATC	Reverse primer for region 950 bp downstream of *sigB* CDS
oIB-53	CTTTAAAACAGTAGGTCAATACTTTTTTTATAT	Reverse primer to verify *sigB* CDS deletion
oIB-76	AAAATATAAAAAAAGTATTGACCTACTGTTTTAAAGATGGTATA GTATTAC	Forward primer to verify *sigB* deletion
oIB-78	GGAGATGTTAACTAATGAATGCATGG	Forward primer to verify *sigB* CDS deletion
oIB-79	CTAATGCACAGCGCCAGCAAACAAAC	Reverse primer to verify *sigB* CDS deletion
oIB-80	ctagcataaaaataagaagcctgcatttgcAAATTTACGAAAAGCTTGC	Forward primer for P_{CD0350}
oIB-82	ctagcataaaaataagaagcctgcatttgcTTGTGTTTAAGGGATTTTGAAAG	Forward primer for P_{CD2963}
oIB-92	ctagcataaaaataagaagcctgcatttgcGAATAAAAAAGGTGGTGTC	Forward primer for P_{CD3614}
oIB-94	agctattaataatttttttacttggtctcatTTTTACCTCCATGTAACATTTATTG	Reverse primer for P_{CD0350}
oIB-95	agctattaataatttttttacttggtctcatAATTAAATCCTTCCTTACATTGT AATTAC	Reverse primer for P_{CD2963}
oIB-100	agctattaataatttttttacttggtctcatATAAACACCCTCCTATTCTTTG	Reverse primer for P_{CD3614}
oPH-19	ctagcataaaaataagaagcctgcatttgcCGATTGCCAAAATAAAT ATTGAAG	Forward primer for P_{CD0007}
oPH-20	agctattaataatttttttacttggtctcatAACAATTACTCCTTTCAATTTT AAATTTTTATC	Reverse primer for P_{CD0007}
oWKS-1240	CACCTCCTTTTTGACTTTAAGCCTACGAATACC	Forward primer on pAP24 backbone to amplify insert
oWKS-1241	CACCGACGAGCAAGGCAAGACCG	Reverse primer on pAP24 backbone to amplify insert
oWKS-1537	TAGGGTAACAAAAAACACCG	Reverse primer to amplify pMTL-SC7315 backbone
oWKS-1538	CCTTTTTGATAATCTCATGACC	Forward primer to amplify pMTL-SC7315 backbone
oWKS-1580	ATGAGACCAAGTAAAAAATTATTAATAGC	Forward primer to amplify pAP24 backbone
oWKS-1582	GCAAATGCAGGCTTCTTATTTTTATG	Reverse primer to amplify pAP24 backbone

[a]Restriction sites are underlined. Overlap with the vector backbone is indicated in lowercase letters.

cells were normalized to the *oriC*/*terC* ratio of DNA samples (3 biological replicates) from nontreated cells. Calculations were performed in Microsoft Office Excel 2010, plotted using Prism 7 (GraphPad), and prepared for publication in Corel Draw Suite X8. Significance was determined using a one-way analysis of variance (ANOVA) and Tukey's test for multiple comparisons (GraphPad).

Growth and RNA isolation for RNA-Seq. For RNA-Seq analysis, *C. difficile* 630Δ*erm* (30, 31) was grown for 5 h in BHI medium with HPUra (35 μg/ml) or ACX-362E (4 μg/ml) starting from an OD_{600} of 0.05 using an exponentially growing starter culture, after which cells (3 ml) were harvested for RNA isolation. These concentrations were some of the highest concentrations that resulted in a modest effects on growth (<30% reduction of growth compared to wild-type cells; Fig. S1). RNA isolation was performed with NucleoSpin RNA kit (Macherey-Nagel). Although the kit includes on column recombinant DNase (rDNase) digestion, a second treatment was performed in solution, and RNA was precipitated and recovered by NaAc precipitation to remove residual DNA. Concentration determination and quality control (16S/23S ratio and RNA integrity number [RIN]) were performed with a fragment analyzer (Agilent Bioanalyzer), according to the instructions of the manufacturer. Samples with an RIN of >9 and 16S/23S rRNA ratio of >1.4 were submitted for analysis by RNA-Seq.

RNA-Seq. RNA-Seq was performed at a commercial provider (GenomeScan, Leiden, The Netherlands). In short, the NEBNext Ultra directional RNA library prep kit for Illumina was used to process the samples. Sample preparation was performed according to the protocol NEBNext Ultra directional RNA library prep kit for Illumina (catalog no. E7420S/L; NEB). Briefly, after selective removal of rRNA (Ribo-Zero

rRNA removal kit for Gram-positive bacteria) and fragmentation of the mRNA, cDNA synthesis was performed. cDNA was ligated to the sequencing adapters, and the resulting product was PCR amplified. Clustering and DNA sequencing using the Illumina NextSeq 500 platform were performed according to the manufacturer's protocols. A concentration of 1.5 pM DNA was used. Image analysis, base calling, and quality check were performed with the Illumina data analysis pipeline RTA version I.18.64 and Bcl2fastq version 2.17. Per sample, four technical replicates were included in the RNA-Seq experiment. In case of insufficient reads, the sample was rerun on another flow cell to reach satisfactory quantities (≥20 million).

Analysis of RNA-Seq data. Analysis of the data was performed using T-REx, a user-friendly web server which has been optimized for the analysis of prokaryotic RNA-Seq-derived expression data (66). The pipeline requires raw RNA expression level data as an input for RNA-Seq data analysis. For data normalization and determination of the genes, the factorial design statistical method of the RNA-Seq analysis R package EdgeR is implemented in the T-REx pipeline. Some samples displayed incomplete rRNA depletion, and rRNA mapping reads had to be removed manually prior to analysis.

To analyze the genome-wide pattern in differential gene expression, a sliding window analysis was performed essentially as described previously (23). In short, genome locations (start of the locus tag) were coupled to the locus tags in the T-REx output. Next, the median log fold change [log(FC)] was calculated for bins of 51 loci, with a step size of 1. For each bin of [X_1, X_2. . .X_{51}], the median absolute deviation of the median [MAD = median(|X_i − median(X)|] was calculated as an robust indication of the distribution around calculated median values. Calculations were performed, three curves (median, median − MAD, and median + MAD) were plotted in Microsoft Office Excel 2010, and the graph was prepared for publication using Adobe Photoshop CC and Corel Draw Suite X8.

A GSEA (33) was performed via the Genome2D web server (66) using our reference genome sequence for *C. difficile* 630Δ*erm* (GenBank accession no. LN614756.1 [listed in Genome2D as "Clostridioides_difficile_630Derm"]) (31). As input, a single list of locus tags was used of either up- or downregulated genes. The output was copied to Microsoft Excel 2010. The single-list column was split, and a column was inserted to calculate the significance of the overrepresentation using the formula "(# hits in list/ClassSize) × −log(*P* value; 2)" to allow for sorting of the output of the GSEA by significance.

General molecular biological techniques. *E. coli* strain DH5α was used for maintenance of all plasmids. All plasmid transformations into *E. coli* were performed using standard procedures (67). *E. coli* CA434 was used as a donor for conjugation of plasmids into the recipient *C. difficile* strain (68). Conjugation was performed as previously described (68). Briefly, 1 ml of an overnight culture of donor cells was mixed with 200 μl of the recipient, spotted onto anaerobic BHI agar plates, and incubated for 5 to 8 h. After incubation, cells were collected, and 10-fold serial dilutions were plated onto fresh BHI plates containing thiamphenicol and CDSS.

Plasmid DNA was isolated using the NucleoSpin plasmid miniprep kits (Macherey-Nagel), as per the manufacturer's instructions. *C. difficile* genomic DNA was isolated using the DNeasy blood and tissue kit (Qiagen), with pretreatment for Gram positives according to the instructions of the manufacturer.

Construction of luciferase-reporter fusion plasmids. All PCRs for plasmid construction were carried out with Q5 polymerase (New England BioLabs). Putative promoter regions were amplified using *C. difficile* 630Δ*erm* chromosomal DNA (31) as the template.

The P_{CD3412} luciferase-reporter plasmid was created by restriction-ligation using the restriction enzymes KpnI and SacI. P_{CD3412} was amplified using primers oIB-26 and oIB-27 (Table 5). The resulting double-stranded DNA (dsDNA) fragment was digested and ligated into KpnI-SacI-digested pAP24 (43), yielding plasmid pIB27. Plasmids pIB68 (P_{CD0350}), pIB69 (P_{CD2963}), pIB74 (P_{CD3614}), and pPH28 (P_{CD0007}) were constructed using a Gibson assembly (69). The plasmid backbone of pAP24 was linearized by PCR using primers oWKS-1580/oWKS-1582, and the predicted promoter areas of CD0350, CD2962, CD3614, and CD0007 were amplified with primers oIB-80/oIB-94, oIB-82/oIB-95, oIB-92/oIB-100, and oPH-19/oPH-20, respectively. Primers were designed using the NEBuilder assembly tool version 1.12.17 (New England BioLabs) using a 30-bp overlap. For the assembly, 100 ng of vector DNA was assembled to a 5-fold molar excess of the PCR fragment of the desired promoter using a homemade Gibson Assembly master mix at 50°C for 30 min (final concentrations, 4 U/μl *Taq* ligase [Westburg], 0.004 U/μl T5 exonuclease [New England BioLabs], 0.025 U/μl Phusion polymerase [Bioké], 5% polyethylene glycol 8000 [PEG-8000], 10 mM $MgCl_2$, 100 mM Tris-HCl [pH 7.5], 10 mM dithiothreitol, 0.2 mM dATP, 0.2 mM dTTP, 0.2 mM dCTP, 0.2 mM dGTP, and 1 mM β-NAD) and transformed into *E. coli* DH5α. Transformants were screened by colony PCR using primers oWKS-1240/oWKS-1241. Transformants yielding PCR fragments of the correct size were verified by Sanger sequencing.

Construction of *C. difficile* IB56 (Δ*sigB*). The up- and downstream regions (950 bp each) of the *sigB* coding sequence were amplified with primers oIB-44/oIB-45 and oIB-46/oIB-47, respectively. Vector pMTL-SC7315 (42) was linearized by PCR using primers oWKS-1537/oWKS-1538. Assembly was done according to the method of Gibson (43, 69). The assembled plasmid was transformed into *E. coli* DH5α and verified using PCR and Sanger sequencing. Generation of the unmarked *sigB* deletion mutant was performed using allele-coupled exchange, essentially as described previously (42, 70). Briefly, pIB54 was introduced into *C. difficile* 630Δ*erm* (31) by conjugation. Transconjugants were grown for 2 days on BHI agar plates supplemented with yeast extract, thiamphenicol, and CDSS, struck onto fresh prereduced plates, and incubated anaerobically at 37°C for 2 days. Single-crossover integration was confirmed using PCR, and those clones were plated onto nonselective BHI agar plates to allow the second crossover event to occur. Colonies were then serially diluted and plated onto minimal agar supplemented with 50 μg/ml 5-fluorocytosine (Sigma), as described previously (42). DNA was isolated from thiamphenicol-susceptible

colonies, and the chromosomal deletion was verified by PCR using primers oIB-78/oIB-79 (Fig. S3), as well as Sanger sequencing of the PCR product using primers oIB-53/oIB-76/oIB-78.

Luciferase reporter assay. Strains containing luciferase reporter plasmids were inoculated to an OD_{600} of 0.05 from an exponentially growing starter culture. Fresh inocula were grown in BHI broth supplemented with yeast extract, with or without 4 μg/ml ACX-362E for 5 h (for putative *sigB* target genes) or 5.5 h (*sigB* promoter). The supernatants from 1 ml of culture (harvested by centrifugation for 10 min, 4°C, 8,000 rpm) were analyzed in a GloMax-Multi microplate multimode reader (Promega), as described before (43). Statistical significance of the data ($P < 0.05$) was determined by two-way analysis of variance (ANOVA) and a pairwise Tukey-Kramer test using Prism 7 (GraphPad) where appropriate.

Data availability. Data for the RNA-Seq experiment have been deposited in the Gene Expression Omnibus (GEO) database (https://www.ncbi.nlm.nih.gov/geo/) under accession number GSE116503 and under GenBank accession number LN614756.1.

SUPPLEMENTAL MATERIAL

Supplemental material for this article may be found at https://doi.org/10.1128/AAC.01363-18.

SUPPLEMENTAL FILE 1, PDF file, 0.26 MB.
SUPPLEMENTAL FILE 2, XLS file, 0.07 MB.
SUPPLEMENTAL FILE 3, XLSX file, 0.07 MB.
SUPPLEMENTAL FILE 4, XLSX file, 0.01 MB.

ACKNOWLEDGMENTS

This work was supported, in part, by a VIDI fellowship (864.13.003) from the Netherlands Organization for Scientific Research, a Gisela Thier Fellowship from the Leiden University Medical Center, and intramural funds to W.K.S.

Anne de Jong is acknowledged for expert assistance with the RNA-Seq analysis, Els Wessels for assistance in designing the MFA real-time PCR, and Jelle Slager for helpful suggestions for the sliding window analysis.

E.V.E. and W.K.S. have performed research for Cubist. E.J.K. has performed research for Cubist, Novartis, and Qiagen, has participated in advisory forums of Astellas, Optimer, Actelion, Pfizer, Sanofi Pasteur, and Seres Therapeutics, and currently holds an unrestricted research grant from Vedanta Biosciences, Inc. G.W. is a consultant for Acurx Pharmaceuticals. The companies had no role in the design of the experiments or the decision to publish. I.M.B. and I.M.J.G.B.-S. declare no conflicts of interest.

E.V.E., I.M.B., E.J.K., and W.K.S. designed the experiments. G.W. and E.J.K. provided reagents or strains. E.V.E., I.M.B., and I.M.J.G.B.-S. performed the experiments. E.V.E., I.M.B., and W.K.S. analyzed the data. E.V.E., I.M.B., and W.K.S. wrote the manuscript. All authors read and approved the final manuscript.

REFERENCES

1. Lawson PA, Citron DM, Tyrrell KL, Finegold SM. 2016. Reclassification of Clostridium difficile as Clostridioides difficile (Hall and O'Toole 1935) Prevot 1938. Anaerobe 40:95–99. https://doi.org/10.1016/j.anaerobe.2016.06.008.
2. Leffler DA, Lamont JT. 2015. Clostridium difficile infection. N Engl J Med 372:1539–1548. https://doi.org/10.1056/NEJMra1403772.
3. Smits WK, Lyras D, Lacy DB, Wilcox MH, Kuijper EJ. 2016. Clostridium difficile infection. Nat Rev Dis Primers 2:16020. https://doi.org/10.1038/nrdp.2016.20.
4. Abt MC, McKenney PT, Pamer EG. 2016. Clostridium difficile colitis: pathogenesis and host defence. Nat Rev Microbiol 14:609–620. https://doi.org/10.1038/nrmicro.2016.108.
5. Commission for Healthcare Audit and Inspection. 2006. Investigation into outbreaks of Clostridium difficile at Stoke Mandeville Hospital, Buckinghamshire Hospitals NHS Trust. Commission for Healthcare Audit and Inspection, London, United Kingdom. https://www.buckshealthcare.nhs.uk/Downloads/healthcarecommision/HCC-Investigation-into-the-Outbreak-of-Clostridium-Difficile.pdf.
6. Bauer MP, Notermans DW, van Benthem BH, Brazier JS, Wilcox MH, Rupnik M, Monnet DL, van Dissel JT, Kuijper EJ, ECIDS Study Group. 2011. Clostridium difficile infection in Europe: a hospital-based survey. Lancet 377:63–73. https://doi.org/10.1016/S0140-6736(10)61266-4.
7. Hensgens MP, Goorhuis A, Dekkers OM, Kuijper EJ. 2012. Time interval of increased risk for Clostridium difficile infection after exposure to antibiotics. J Antimicrob Chemother 67:742–748. https://doi.org/10.1093/jac/dkr508.
8. He M, Miyajima F, Roberts P, Ellison L, Pickard DJ, Martin MJ, Connor TR, Harris SR, Fairley D, Bamford KB, D'Arc S, Brazier J, Brown D, Coia JE, Douce G, Gerding D, Kim HJ, Koh TH, Kato H, Senoh M, Louie T, Michell S, Butt E, Peacock SJ, Brown NM, Riley T, Songer G, Wilcox M, Pirmohamed M, Kuijper E, Hawkey P, Wren BW, Dougan G, Parkhill J, Lawley TD. 2013. Emergence and global spread of epidemic healthcare-associated Clostridium difficile. Nat Genet 45:109–113. https://doi.org/10.1038/ng.2478.
9. Debast SB, Bauer MP, Kuijper EJ, European Society Of CM, Infectious D. 2014. European Society of Clinical Microbiology and Infectious Diseases: update of the treatment guidance document for Clostridium difficile infection. Clin Microbiol Infect 20:1–26. https://doi.org/10.1111/1469-0691.12418.
10. McDonald LC, Gerding DN, Johnson S, Bakken JS, Carroll KC, Coffin SE, Dubberke ER, Garey KW, Gould CV, Kelly C, Loo V, Shaklee Sammons J, Sandora TJ, Wilcox MH. 2018. Clinical practice guidelines for Clostridium difficile infection in adults and children: 2017 update by the Infectious Diseases Society of America (IDSA) and Society for Healthcare Epidemiology of America (SHEA). Clin Infect Dis 66:e1–e48. https://doi.org/10.1093/cid/cix1085.
11. Baines SD, O'Connor R, Freeman J, Fawley WN, Harmanus C, Mastranto-

nio P, Kuijper EJ, Wilcox MH. 2008. Emergence of reduced susceptibility to metronidazole in Clostridium difficile. J Antimicrob Chemother 62:1046–1052. https://doi.org/10.1093/jac/dkn313.
12. Chong PM, Lynch T, McCorrister S, Kibsey P, Miller M, Gravel D, Westmacott GR, Mulvey MR, Canadian Nosocomial Infection Surveillance Program (CNISP). 2014. Proteomic analysis of a NAP1 Clostridium difficile clinical isolate resistant to metronidazole. PLoS One 9:e82622. https://doi.org/10.1371/journal.pone.0082622.
13. Moura I, Spigaglia P, Barbanti F, Mastrantonio P. 2013. Analysis of metronidazole susceptibility in different Clostridium difficile PCR ribotypes. J Antimicrob Chemother 68:362–365. https://doi.org/10.1093/jac/dks420.
14. Davies J, Spiegelman GB, Yim G. 2006. The world of subinhibitory antibiotic concentrations. Curr Opin Microbiol 9:445–453. https://doi.org/10.1016/j.mib.2006.08.006.
15. Slager J, Veening JW. 2016. Hard-wired control of bacterial processes by chromosomal gene location. Trends Microbiol 24:788–800. https://doi.org/10.1016/j.tim.2016.06.003.
16. Tarantino PM, Jr, Zhi C, Wright GE, Brown NC. 1999. Inhibitors of DNA polymerase III as novel antimicrobial agents against gram-positive eubacteria. Antimicrob Agents Chemother 43:1982–1987. https://doi.org/10.1128/AAC.43.8.1982.
17. Brown NC. 1970. 6-(*p*-Hydroxyphenylazo)-uracil: a selective inhibitor of host DNA replication in phage-infected Bacillus subtilis. Proc Natl Acad Sci U S A 67:1454–1461. https://doi.org/10.1073/pnas.67.3.1454.
18. Butler MM, Dudycz LW, Khan NN, Wright GE, Brown NC. 1990. Development of novel inhibitor probes of DNA polymerase III based on dGTP analogs of the HPUra type: base, nucleoside and nucleotide derivatives of N_2-(3,4-dichlorobenzyl)guanine. Nucleic Acids Res 18:7381–7387. https://doi.org/10.1093/nar/18.24.7381.
19. Torti A, Lossani A, Savi L, Focher F, Wright GE, Brown NC, Xu WC. 2011. Clostridium difficile DNA polymerase IIIC: basis for activity of antibacterial compounds. Curr Enzym Inhib 7:147–153. https://doi.org/10.2174/157340811798807597.
20. Dvoskin S, Xu WC, Brown NC, Yanachkov IB, Yanachkova M, Wright GE. 2012. A novel agent effective against Clostridium difficile infection. Antimicrob Agents Chemother 56:1624–1626. https://doi.org/10.1128/AAC.06097-11.
21. Goranov AI, Katz L, Breier AM, Burge CB, Grossman AD. 2005. A transcriptional response to replication status mediated by the conserved bacterial replication protein DnaA. Proc Natl Acad Sci U S A 102:12932–12937. https://doi.org/10.1073/pnas.0506174102.
22. Goranov AI, Kuester-Schoeck E, Wang JD, Grossman AD. 2006. Characterization of the global transcriptional responses to different types of DNA damage and disruption of replication in Bacillus subtilis. J Bacteriol 188:5595–5605. https://doi.org/10.1128/JB.00342-06.
23. Slager J, Kjos M, Attaiech L, Veening JW. 2014. Antibiotic-induced replication stress triggers bacterial competence by increasing gene dosage near the origin. Cell 157:395–406. https://doi.org/10.1016/j.cell.2014.01.068.
24. Knetsch CW, Terveer EM, Lauber C, Gorbalenya AE, Harmanus C, Kuijper EJ, Corver J, van Leeuwen HC. 2012. Comparative analysis of an expanded Clostridium difficile reference strain collection reveals genetic diversity and evolution through six lineages. Infect Genet Evol 12:1577–1585. https://doi.org/10.1016/j.meegid.2012.06.003.
25. He M, Sebaihia M, Lawley TD, Stabler RA, Dawson LF, Martin MJ, Holt KE, Seth-Smith HM, Quail MA, Rance R, Brooks K, Churcher C, Harris D, Bentley SD, Burrows C, Clark L, Corton C, Murray V, Rose G, Thurston S, van Tonder A, Walker D, Wren BW, Dougan G, Parkhill J. 2010. Evolutionary dynamics of Clostridium difficile over short and long time scales. Proc Natl Acad Sci U S A 107:7527–7532. https://doi.org/10.1073/pnas.0914322107.
26. CLSI. 2012. Methods for antimicrobial susceptibility testing of anaerobic bacteria; approved standard, 8th ed. CLSI document M11-A8. Clinical and Laboratory Standards Institute, Wayne, PA.
27. Freeman J, Stott J, Baines SD, Fawley WN, Wilcox MH. 2005. Surveillance for resistance to metronidazole and vancomycin in genotypically distinct and UK epidemic Clostridium difficile isolates in a large teaching hospital. J Antimicrob Chemother 56:988–989. https://doi.org/10.1093/jac/dki357.
28. Debast SB, Bauer MP, Sanders IM, Wilcox MH, Kuijper EJ, ECDIS Study Group. 2013. Antimicrobial activity of LFF571 and three treatment agents against Clostridium difficile isolates collected for a pan-European survey in 2008: clinical and therapeutic implications. J Antimicrob Chemother 68:1305–1311. https://doi.org/10.1093/jac/dkt013.
29. Pacitti DF, Barnes MH, Li DH, Brown NC. 1995. Characterization and overexpression of the gene encoding Staphylococcus aureus DNA polymerase III. Gene 165:51–56. https://doi.org/10.1016/0378-1119(95)00377-I.
30. Hussain HA, Roberts AP, Mullany P. 2005. Generation of an erythromycin-sensitive derivative of Clostridium difficile strain 630 (630Δerm) and demonstration that the conjugative transposon Tn916ΔE enters the genome of this strain at multiple sites. J Med Microbiol 54:137–141. https://doi.org/10.1099/jmm.0.45790-0.
31. van Eijk E, Anvar SY, Browne HP, Leung WY, Frank J, Schmitz AM, Roberts AP, Smits WK. 2015. Complete genome sequence of the Clostridium difficile laboratory strain 630Δerm reveals differences from strain 630, including translocation of the mobile element CTn5. BMC Genomics 16:31. https://doi.org/10.1186/s12864-015-1252-7.
32. Hastey CJ, Dale SE, Nary J, Citron D, Law JH, Roe-Carpenter DE, Chesnel L. 2017. Comparison of Clostridium difficile minimum inhibitory concentrations obtained using agar dilution vs broth microdilution methods. Anaerobe 44:73–77. https://doi.org/10.1016/j.anaerobe.2017.02.006.
33. Subramanian A, Tamayo P, Mootha VK, Mukherjee S, Ebert BL, Gillette MA, Paulovich A, Pomeroy SL, Golub TR, Lander ES, Mesirov JP. 2005. Gene set enrichment analysis: a knowledge-based approach for interpreting genome-wide expression profiles. Proc Natl Acad Sci U S A 102:15545–15550. https://doi.org/10.1073/pnas.0506580102.
34. van Eijk E, Paschalis V, Green M, Friggen AH, Larson MA, Spriggs K, Briggs GS, Soultanas P, Smits WK. 2016. Primase is required for helicase activity and helicase alters the specificity of primase in the enteropathogen Clostridium difficile. Open Biol 6:160272. https://doi.org/10.1098/rsob.160272.
35. Sousa C, de Lorenzo V, Cebolla A. 1997. Modulation of gene expression through chromosomal positioning in Escherichia coli. Microbiology 143:2071–2078. https://doi.org/10.1099/00221287-143-6-2071.
36. Sauer C, Syvertsson S, Bohorquez LC, Cruz R, Harwood CR, van Rij T, Hamoen LW. 2016. Effect of genome position on heterologous gene expression in Bacillus subtilis: an unbiased analysis. ACS Synth Biol 5:942–947. https://doi.org/10.1021/acssynbio.6b00065.
37. Block DH, Hussein R, Liang LW, Lim HN. 2012. Regulatory consequences of gene translocation in bacteria. Nucleic Acids Res 40:8979–8992. https://doi.org/10.1093/nar/gks694.
38. Samadpour AN, Merrikh H. 2018. DNA gyrase activity regulates DnaA-dependent replication initiation in Bacillus subtilis. Mol Microbiol 108:115–127. https://doi.org/10.1111/mmi.13920.
39. Sebaihia M, Wren BW, Mullany P, Fairweather NF, Minton N, Stabler R, Thomson NR, Roberts AP, Cerdeno-Tarraga AM, Wang H, Holden MT, Wright A, Churcher C, Quail MA, Baker S, Bason N, Brooks K, Chillingworth T, Cronin A, Davis P, Dowd L, Fraser A, Feltwell T, Hance Z, Holroyd S, Jagels K, Moule S, Mungall K, Price C, Rabbinowitsch E, Sharp S, Simmonds M, Stevens K, Unwin L, Whithead S, Dupuy B, Dougan G, Barrell B, Parkhill J. 2006. The multidrug-resistant human pathogen Clostridium difficile has a highly mobile, mosaic genome. Nat Genet 38:779–786. https://doi.org/10.1038/ng1830.
40. Kint N, Janoir C, Monot M, Hoys S, Soutourina O, Dupuy B, Martin-Verstraete I. 2017. The alternative sigma factor sigma(B) plays a crucial role in adaptive strategies of Clostridium difficile during gut infection. Environ Microbiol 19:1933–1958. https://doi.org/10.1111/1462-2920.13696.
41. Hecker M, Pané-Farré J, Völker U. 2007. SigB-dependent general stress response in Bacillus subtilis and related Gram-positive bacteria. Annu Rev Microbiol 61:215–236. https://doi.org/10.1146/annurev.micro.61.080706.093445.
42. Cartman ST, Kelly ML, Heeg D, Heap JT, Minton NP. 2012. Precise manipulation of the Clostridium difficile chromosome reveals a lack of association between the tcdC genotype and toxin production. Appl Environ Microbiol 78:4683–4690. https://doi.org/10.1128/AEM.00249-12.
43. Oliveira Paiva AM, Friggen AH, Hossein-Javaheri S, Smits WK. 2016. The signal sequence of the abundant extracellular metalloprotease PPEP-1 can be used to secrete synthetic reporter proteins in Clostridium difficile. ACS Synth Biol 5:1376–1382. https://doi.org/10.1021/acssynbio.6b00104.
44. Lynch T, Chong P, Zhang J, Hizon R, Du T, Graham MR, Beniac DR, Booth TF, Kibsey P, Miller M, Gravel D, Mulvey MR, Canadian Nosocomial Infection Surveillance Program (CNISP). 2013. Characterization of a stable, metronidazole-resistant Clostridium difficile clinical isolate. PLoS One 8:e53757. https://doi.org/10.1371/journal.pone.0053757.
45. Goldstein EJ, Citron DM, Sears P, Babakhani F, Sambol SP, Gerding DN. 2011. Comparative susceptibilities to fidaxomicin (OPT-80) of isolates collected at baseline, recurrence, and failure from patients in two phase III trials of

fidaxomicin against Clostridium difficile infection. Antimicrob Agents Chemother 55:5194–5199. https://doi.org/10.1128/AAC.00625-11.
46. Knetsch CW, Kumar N, Forster SC, Connor TR, Browne HP, Harmanus C, Sanders IM, Harris SR, Turner L, Morris T, Perry M, Miyajima F, Roberts P, Pirmohamed M, Songer JG, Weese JS, Indra A, Corver J, Rupnik M, Wren BW, Riley TV, Kuijper EJ, Lawley TD. 2018. Zoonotic transfer of Clostridium difficile harboring antimicrobial resistance between farm animals and humans. J Clin Microbiol 56:e01384-17. https://doi.org/10.1128/JCM.01384-17.
47. Ott RW, Barnes MH, Brown NC, Ganesan AT. 1986. Cloning and characterization of the polC region of Bacillus subtilis. J Bacteriol 165:951–957. https://doi.org/10.1128/jb.165.3.951-957.1986.
48. Barnes MH, Hammond RA, Foster KA, Mitchener JA, Brown NC. 1989. The cloned polC gene of Bacillus subtilis: characterization of the azp12 mutation and controlled in vitro synthesis of active DNA polymerase III. Gene 85:177–186. https://doi.org/10.1016/0378-1119(89)90478-2.
49. Barnes MH, Hammond RA, Kennedy CC, Mack SL, Brown NC. 1992. Localization of the exonuclease and polymerase domains of Bacillus subtilis DNA polymerase III. Gene 111:43–49. https://doi.org/10.1016/0378-1119(92)90601-K.
50. Barnes MH, Butler MM, Wright GE, Brown NC. 2012. Antimicrobials targeted to the replication-specific DNA polymerases of gram-positive bacteria: target potential of dnaE. Infect Disord Drug Targets 12:327–331. https://doi.org/10.2174/187152612804142279.
51. Timinskas K, Balvočiūtė M, Timinskas A, Venclovas Č. 2014. Comprehensive analysis of DNA polymerase III alpha subunits and their homologs in bacterial genomes. Nucleic Acids Res 42:1393–1413. https://doi.org/10.1093/nar/gkt900.
52. Wecke T, Mascher T. 2011. Antibiotic research in the age of omics: from expression profiles to interspecies communication. J Antimicrob Chemother 66:2689–2704. https://doi.org/10.1093/jac/dkr373.
53. Kazmierczak MJ, Mithoe SC, Boor KJ, Wiedmann M. 2003. Listeria monocytogenes sigma B regulates stress response and virulence functions. J Bacteriol 185:5722–5734. https://doi.org/10.1128/JB.185.19.5722-5734.2003.
54. Weber H, Polen T, Heuveling J, Wendisch VF, Hengge R. 2005. Genome-wide analysis of the general stress response network in Escherichia coli: sigmaS-dependent genes, promoters, and sigma factor selectivity. J Bacteriol 187:1591–1603. https://doi.org/10.1128/JB.187.5.1591-1603.2005.
55. van Schaik W, van der Voort M, Molenaar D, Moezelaar R, de Vos WM, Abee T. 2007. Identification of the sigmaB regulon of Bacillus cereus and conservation of sigmaB-regulated genes in low-GC-content Gram-positive bacteria. J Bacteriol 189:4384–4390. https://doi.org/10.1128/JB.00313-07.
56. Kreuzer KN. 2013. DNA damage responses in prokaryotes: regulating gene expression, modulating growth patterns, and manipulating replication forks. Cold Spring Harb Perspect Biol 5:a012674. https://doi.org/10.1101/cshperspect.a012674.
57. Helmann JD, Wu MF, Kobel PA, Gamo FJ, Wilson M, Morshedi MM, Navre M, Paddon C. 2001. Global transcriptional response of Bacillus subtilis to heat shock. J Bacteriol 183:7318–7328. https://doi.org/10.1128/JB.183.24.7318-7328.2001.
58. Ternan NG, Jain S, Srivastava M, McMullan G. 2012. Comparative transcriptional analysis of clinically relevant heat stress response in Clostridium difficile strain 630. PLoS One 7:e42410. https://doi.org/10.1371/journal.pone.0042410.
59. Emerson JE, Stabler RA, Wren BW, Fairweather NF. 2008. Microarray analysis of the transcriptional responses of Clostridium difficile to environmental and antibiotic stress. J Med Microbiol 57:757–764. https://doi.org/10.1099/jmm.0.47657-0.
60. Walter BM, Rupnik M, Hodnik V, Anderluh G, Dupuy B, Paulic N, Zgur-Bertok D, Butala M. 2014. The LexA regulated genes of the Clostridium difficile. BMC Microbiol 14:88. https://doi.org/10.1186/1471-2180-14-88.
61. Couturier E, Rocha EP. 2006. Replication-associated gene dosage effects shape the genomes of fast-growing bacteria but only for transcription and translation genes. Mol Microbiol 59:1506–1518. https://doi.org/10.1111/j.1365-2958.2006.05046.x.
62. Bidet P, Lalande V, Salauze B, Burghoffer B, Avesani V, Delmee M, Rossier A, Barbut F, Petit JC. 2000. Comparison of PCR-ribotyping, arbitrarily primed PCR, and pulsed-field gel electrophoresis for typing Clostridium difficile. J Clin Microbiol 38:2484–2487.
63. Kato H, Kato N, Watanabe K, Iwai N, Nakamura H, Yamamoto T, Suzuki K, Kim SM, Chong Y, Wasito EB. 1998. Identification of toxin A-negative, toxin B-positive Clostridium difficile by PCR. J Clin Microbiol 36:2178–2182.
64. Paltansing S, van den Berg RJ, Guseinova RA, Visser CE, van der Vorm ER, Kuijper EJ. 2007. Characteristics and incidence of Clostridium difficile-associated disease in The Netherlands, 2005. Clin Microbiol Infect 13:1058–1064. https://doi.org/10.1111/j.1469-0691.2007.01793.x.
65. Stubbs S, Rupnik M, Gibert M, Brazier J, Duerden B, Popoff M. 2000. Production of actin-specific ADP-ribosyltransferase (binary toxin) by strains of Clostridium difficile. FEMS Microbiol Lett 186:307–312. https://doi.org/10.1111/j.1574-6968.2000.tb09122.x.
66. de Jong A, van der Meulen S, Kuipers OP, Kok J. 2015. T-REx: transcriptome analysis webserver for RNA-seq expression data. BMC Genomics 16:663. https://doi.org/10.1186/s12864-015-1834-4.
67. Sambrook J, Russell DW. 2001. Molecular cloning: a laboratory manual. Cold Spring Harbor Laboratory, Cold Spring Harbor, NY.
68. Purdy D, O'Keeffe TA, Elmore M, Herbert M, McLeod A, Bokori-Brown M, Ostrowski A, Minton NP. 2002. Conjugative transfer of clostridial shuttle vectors from Escherichia coli to Clostridium difficile through circumvention of the restriction barrier. Mol Microbiol 46:439–452. https://doi.org/10.1046/j.1365-2958.2002.03134.x.
69. Gibson DG, Young L, Chuang R-Y, Venter JC, Hutchison CA, III, Smith HO. 2009. Enzymatic assembly of DNA molecules up to several hundred kilobases. Nat Methods 6:343–345. https://doi.org/10.1038/nmeth.1318.
70. van Leeuwen PT, van der Peet JM, Bikker FJ, Hoogenkamp MA, Oliveira Paiva AM, Kostidis S, Mayboroda OA, Smits WK, Krom BP. 2016. Interspecies interactions between Clostridium difficile and Candida albicans. mSphere 1:e00187-16. https://doi.org/10.1128/mSphere.00187-16.